

High Resolution Regularized Least Squares AVA Kirchhoff Migration

Jiang Feng and Mauricio D. Sacchi, Department of Physics, University of Alberta

Summary

This paper proposes a strategy to perform amplitude versus angle (AVA) imaging and rock physical properties inversion by applying the conjugate gradient (CG) method on a ray-based Kirchhoff migration/inversion scheme in the angle domain. The idea is to use the Kirchhoff integral formulation to estimate rock physical parameters directly from pre-stack seismic data. To improve the vertical resolution a non-quadratic regularization strategy is also proposed. The implementation of this method shows a successful delineation of subsurface structures and an accurate recovering of local changes in rock physical properties for a 2D model.

Introduction

Imaging using ray based Kirchhoff migration/inversion is a very common application in exploration geophysics (Gray and May, 1994). Nowadays, the goal of migration has changed its focus from imaging subsurface structures to recovering elastic properties (Beydoun and Mendes, 1989). As the rock physical parameters are not related linearly to the seismic reflection data (Lumley and Beydoun, 1997), usually, the inversion for elastic constants is performed in two steps:

- 1) Pre-stack seismic data are transformed to common image gathers (CIGs) by migration or inversion. This step requires a migration algorithm for complex media that preserves amplitudes.
- 2) Using approximations to the Zoeppritz equations (Aki and Richards, 1980; Shuey, 1985; Fatti et al., 1994) transform the CIGs to perturbations of the elastic parameters (Beretta et al., 2002; Li et al., 2003).

Generally, pre-stack migration and AVA (or AVO) analysis technologies are developed by people with different goals in mind, and, consequently, AVO-based analysis of rock properties are rarely incorporated into sophisticated migration procedures (Xu, 2003). Pre-stack migration has great advantages at the time of imaging complex geological structures over other seismic processing schemes. Therefore, integrating AVO and imaging together should lead to a new class of algorithms capable of imaging the Earth's interior and retrieving the physical properties (Downton and Lines, 2003).

Our imaging technique is mainly based on the work developed by Bleistein (1987; 2001; 2002a; 2002b) and Xu et al. (2001) on Kirchhoff migration/inversion. In particular, we implement our algorithm as a regularized least-squares migration problem where we estimate elastic parameter perturbations directly from the pre-stack data volume. Moreover, to obtain high resolution results, a

non-quadratic regularization term, which is expressed as a Cauchy constraint (Ulrych et al., 2001), is used to enforce vertical sparseness.

Methodology

Commonly, a linear scattering problem is described as

$$d = W L m + n, \quad (1)$$

where d denotes the pre-stack seismic data, m refers to the model (CIG gathers), n denotes additive noise, W represents the wavelet, and L represents the Kirchhoff forward operator. In the frequency domain, the above equation can be written as

$$d(\mathbf{s}, \mathbf{r}, \omega) = i\omega \int m(\mathbf{x}, \theta) A(\mathbf{r}, \mathbf{x}, \mathbf{s}) [\mathbf{n} \cdot \nabla \tau(\mathbf{r}, \mathbf{x}, \mathbf{s})] e^{i\omega \tau(\mathbf{r}, \mathbf{x}, \mathbf{s})} W(\omega) d^3 \mathbf{x}, \quad (2)$$

where \mathbf{s} , \mathbf{r} denote the source and receiver position, respectively. The variable ω refers to the angular frequency, θ refers to the reflection angle, the arbitrary space position is defined by \mathbf{x} , A refers to the amplitude (geometrical-spreading factor from source \mathbf{s} to receiver \mathbf{r} via \mathbf{x}) and τ refers to the traveltime. Both A and τ can be calculated by target oriented dynamic ray-tracing on a macro velocity model. Note that the image m is related to the vector of physical parameters p via a Zoeppritz forward operator Z ,

$$m = Z p. \quad (3)$$

For PP reflections, Aki and Richards (1980) provide the following approximation to the Zoeppritz operator

$$m(\mathbf{x}, \theta) = \frac{1}{2} \left(1 - 4 \frac{v_s^2}{v_p^2} \sin^2 \theta \right) \frac{\Delta \rho}{\rho} + \frac{\sec^2 \theta}{2} \frac{\Delta v_p}{v_p} - 4 \frac{v_s^2}{v_p^2} \sin^2 \theta \frac{\Delta v_s}{v_s}, \quad (4)$$

where ρ , v_p , v_s are the average density, P-wave velocity and S-wave velocity of two adjacent layers respectively. Furthermore, $\Delta \rho$, Δv_p , Δv_s are the difference in density, P-wave velocity and S-wave velocity of two adjacent layers respectively. The angle θ is the average of incidence and transmission angles. In the case of negligible difference in the elastic parameters, this angle θ can be approximated by the reflection angle.

High Resolution AVA

Combining equation (1) and equation (3), the seismic data can now be expressed by

$$d = WLZp + n. \quad (5)$$

Since equation (5) lies in the category of ill-posed problems; there is no perfect solution to it, therefore, a constrained least squares approach is used to retrieve a unique and stable solution. Moreover, the Conjugate Gradients (CG) algorithm is used to avoid the calculation of the inverse of large operators generated during least squares inversion (Feng and Sacchi, 2004). The CG method finds a solution by directly minimizing the cost function which, in our case, is the sum of a data space misfit and model space regularization terms.

We then estimate p from d by minimizing the following cost function \mathcal{J} :

$$\begin{aligned} \mathcal{J} = & \left\| d - WLZp \right\|^2 + \mu_1 \left\| \frac{\partial p}{\partial x_1} \right\|^2 + \\ & \mu_2 \left\| \frac{\partial p}{\partial x_2} \right\|^2 + \mu_3 \mathcal{R}(p), \end{aligned} \quad (6)$$

the first term is the misfit, a figure of data reconstruction fidelity, the second and the third terms are first order model derivatives, which enforce a smooth solution along the horizontal plane; the last term, \mathcal{R} , is a Cauchy model norm used to impose vertical sparseness to the final solution or, in other words, to gain vertical resolution (Sacchi, 1997). In addition, the form of the Cauchy norm for an arbitrary vector of parameters x_1, x_2, \dots, x_N is given by

$$\mathcal{R}(x) = \sum_{i=1}^N \ln \left(1 + \frac{x_i^2}{\sigma_c^2} \right),$$

where σ_c is a parameter used to control the degree of sparseness of the solution. Notice that the non-quadratic term (Cauchy norm) leads to a non-linear optimization problem. The minimization of the above cost function requires an important computational effort that we would like to avoid. Thus, equation (6) is rewritten as

$$\begin{aligned} \mathcal{J}_1 = & \left\| d - WLZ\hat{p} \right\|^2 + \mu_1 \left\| \frac{\partial \hat{p}}{\partial x_1} \right\|^2 + \\ & \mu_2 \left\| \frac{\partial \hat{p}}{\partial x_2} \right\|^2 + \mu_3 \|\hat{p}\|^2, \end{aligned} \quad (7)$$

$$\mathcal{J}_2 = \left\| \hat{p} - Cp \right\|^2 + \mu \mathcal{R}(p), \quad (8)$$

where \hat{p} is the smeared solution of p , and C is a time-variant convolutional operator. Equation (7) is minimized using the method of Conjugate Gradients, whereas \mathcal{J}_2 is minimized using a non-linear optimization scheme described in Sacchi (1997). Optimization strategies for a

direct and efficient computational scheme capable of minimizing (6) are under development.

Examples

A 2D acoustic geological model is created to test the accuracy of the proposed inversion (Figure 1A). The model is composed of 7 layers, including a fold, a pinch out and interfaces with topography. The synthetic data set (Table 1) was calculated using a finite-difference modeling program provided by Seismic Unix (Center for Wave Phenomena, Colorado School of Mines). The data are sampled every 4 ms.

Number of Shots	51
Number of Receivers	51 × 201
Shot Spacing (m)	20
Receiver Spacing (m)	20
First shot position (m)	2000
First receiver offset (m)	2000

Table 1: Acquisition geometry for the 2D synthetic model.

The synthetic data set was inverted for physical properties $p = [\Delta v/v, \Delta \rho/\rho]^T$ using the method outlined above. The recovered structural image is clear and correct (Figure 1B and 1C). The common image gather at $x = 3600$ meters (Figure 2A) shows coherent and continuous events for a wide range of reflection angles. Notice that this gather is generated by mapping the parameter vector p to the common image gather panel m using equation (3). This is an important difference with respect to earlier strategies proposed by Kuehl and Sacchi (2003) where lateral smoothness was directly imposed on the common image gather rather than on the vector of parameters p .

The picked AVA (Figure 2B) matches the theoretical values for angles within the domain of illumination. The theoretical equation for the AVA curve (Acoustic PP reflection) is given by

$$R(\theta) = \frac{\rho_2 v_2 \cos \theta_1 - \rho_1 v_1 \cos \theta_2}{\rho_2 v_2 \cos \theta_1 + \rho_1 v_1 \cos \theta_2}, \quad (9)$$

where $R(\theta)$ is angle dependent reflectivity, ρ_1, ρ_2, v_1, v_2 are densities and velocities of upper and lower layers respectively, θ_1, θ_2 are the incident and transmitted angles respectively.

The comparison between the inverted results and true physical properties shows a good agreement with the perturbations computed using the true velocity/density model (Figure 3). As no energy losses due to transmission is included in this algorithm, the accuracy of the inversion degrades for deeper horizons.

Conclusions

We have proposed an AVA and physical parameter inversion algorithm. The main advantages of the proposed method are: 1) structural complexity can be incorporated in the AVA/AVO estimation problem, 2) regularization

High Resolution AVA

methods can be easily incorporated to enhance the spatial continuity of reflectors, 3) acquisition footprints can be minimized by incorporating data space weights (Sacchi and Kuehl, 2003), 4) AVA/AVO analysis can be obtained as a byproduct of pre-stack migration/inversion, and finally, 5) ray based Kirchhoff least-squares migration can be efficiently implemented in a target-oriented scheme.

Acknowledgments

The authors would like to thank the sponsors of the Seismic Analysis and Imaging Group at the University of Alberta: EnCana, Geo-X Ltd, Veritas DGC, AERI-Department of Energy, Province of Alberta, and NSERC for funding this research. In addition, the authors thank Ulrich Theune and Yiqian Wang for their helpful suggestions and proofreading.

References

- Aki, K., and Richards, P. G., 1980, Quantitative Seismology: Theory and Methods: W. H. Freeman and Co.
- Beretta, M., Bernasconi, G., and Drufuca, G., 2002, AVO and AVA inversion for fractured reservoir characterization: *Geophysics*, **67**, 300–306.
- Beydoun, W. B., and Mendes, M., 1989, Elastic ray-Born l_2 -migration/inversion: *Geophys. J.*, **97**, 151–160.
- Bleistein, N., and Gray, S. H., 2002a, From the Hagedoorn imaging technique to Kirchhoff migration and inversion: Website of Center for Wave Phenomena, Colorado School of Mines.
- 2002b, A proposal for common-opening-angle migration/inversion: Website of Center for Wave Phenomena, Colorado School of Mines.
- Bleistein, N., Cohen, J. K., and Stockwell, J. W., 2001, Mathematics of multidimensional seismic imaging, migration, and inversion: Springer.
- Bleistein, N., 1987, On the imaging of reflectors in the earth: *Geophysics*, **52**, 931–942.
- Downton, E. J., and Lines, R. L., 2003, High-resolution AVO NMO: 2003 CSEG National Convention, CSEG.
- Fatti, J. L., Smith, G. C., Vail, P. J., Strauss, P. J., and Levitt, P. R., 1994, Detection of gas in sandstone sandstone reservoirs using AVO analysis: a 3-d seismic case history using the Geostack technique: *Geophysics*, **59**, 1362–1376.
- Feng, J., and Sacchi, M., 2004, Rock properties inversion with Kirchhoff AVA migration/inversion: 2004 CSEG National Convention, CSEG.
- Gray, H. S., and May, P. W., 1994, Kirchhoff migration using Eikonal equation traveltimes: *Geophysics*, **59**, 810–817.
- Kuehl, H., and Sacchi, M., 2003, Least squares wave-equation migration for AVP/AVA inversion: *Geophysics*, **68**, 262–273.
- Li, Y. Y., Goodway, B., and Downton, J., 2003, Recent advances in application of AVO to carbonate reservoirs: *Recorder*, **28**, 34–40.
- Lumley, D. E., and Beydoun, W. B., 1997, Elastic parameter estimation by Kirchhoff prestack depth migration/inversion: SEP report, SEP, 162–190.
- Sacchi, M. D., 1997, Reweighting strategies in seismic deconvolution: *Geophys. J. Int.*, **129**, 651–656.
- Shuey, T. R., 1985, A simplification of the Zoeppritz equations: *Geophysics*, **50**, 609–614.
- Ulrych, T. J., Sacchi, M., and Woodbury, A., 2001, Tutorial: A Bayes tour of inversion: *Geophysics*, **66**, 55–69.
- Xu, S., Chauris, H., Lambaré, G., and Noble, M., 2001, Common-angle migration: A strategy for imaging complex media: *Geophysics*, **66**, 1877–1894.
- Xu, Y., 2003, Angle-dependent amplitude and AVO/AVA analysis with PSDM: 2003 CSEG National Convention, CSEG.

High Resolution AVA

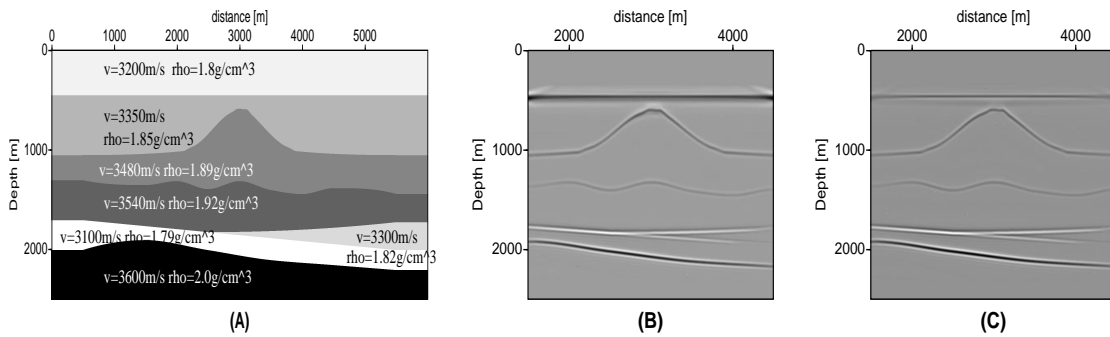


Fig. 1: Acoustic geological model for the synthetic data set (A), and corresponding inverted model for $\frac{\Delta v}{v}$ (B) and $\frac{\Delta \rho}{\rho}$ (C) before applying sparse inversion.

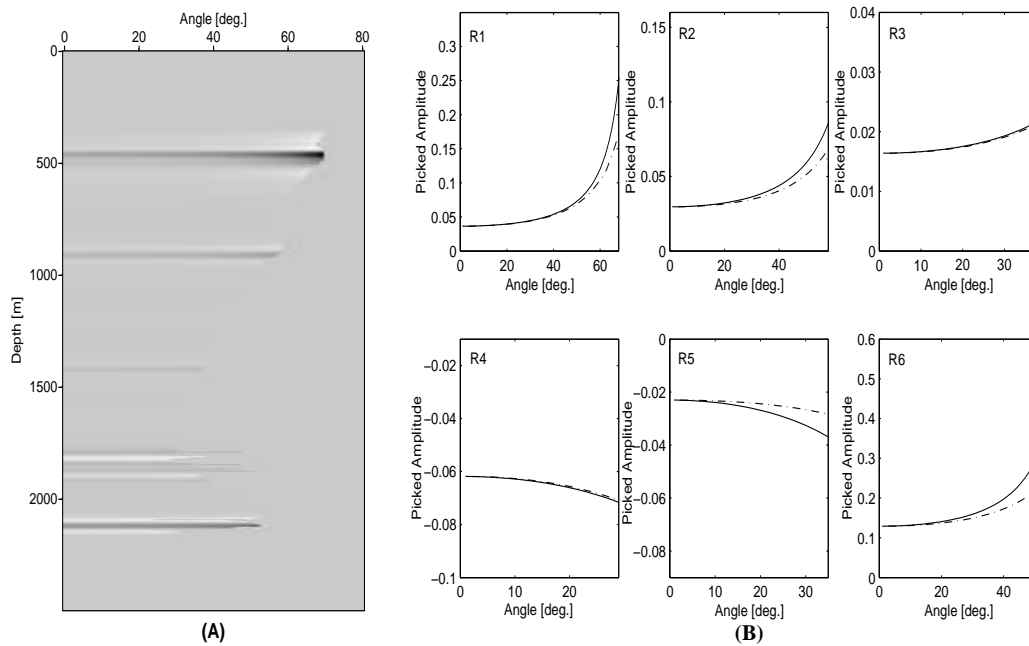


Fig. 2: Inverted CIG of the synthetic data at $x = 3600$ meters (A), and corresponding picked AVA (R1-R6) curves for six layers (B). Dash lines represent the picked AVA curves, solid lines indicate the theoretical curves.

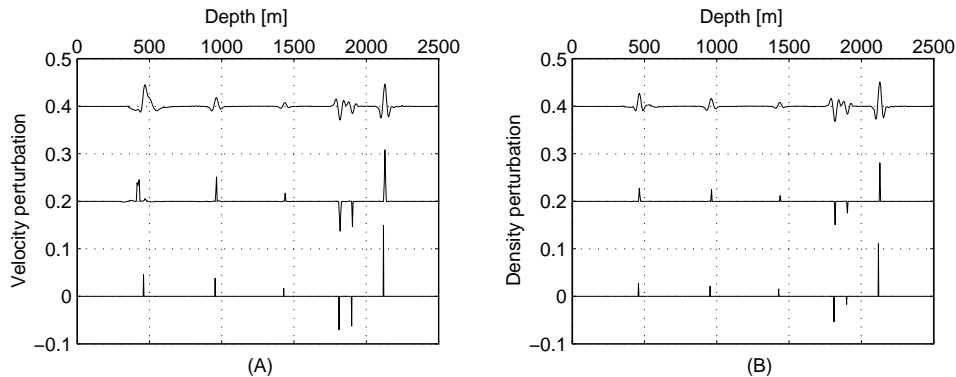


Fig. 3: The comparison between the inverted and true velocity (A), density (B) perturbations at $x = 3700$ meters. The smeared inversion (top), perturbations after sparse inversion, (middle), and the true perturbations (bottom).